



Synthesis, evaluation, and *in silico* studies of 2-mercapto-5-substituted styryl-1,3,4-oxadiazoles as potential cytotoxic agents

Anitha Kumari Vinjavarapu, Shaheen Begum, Bharathi Koganti

Department of Pharmaceutical Chemistry, Institute of Pharmaceutical Technology, Sri Padmavathi Mahila Visvavidyalayam, Tirupati, Andhra Pradesh, India

Corresponding Author:

Anitha Kumari Vinjavarapu,
Institute of Pharmaceutical
Technology, Sri Padmavati
Mahila Visvavidyalayam,
Tirupati - 517 502,
Andhra Pradesh, India.
Phone: +91-9492293877.
Fax no: 08772284531.
E-mail: anithamedchem@
gmail.com

Received: Nov 01, 2019

Accepted: Nov 22, 2019

Published: Dec 31, 2019

ABSTRACT

Objective: The objective of the present study is to design, synthesize and evaluate 2-mercapto-5-styryl-1,3,4-oxadiazoles with an aim of developing potential cytotoxic agents and to carryout *in silico* studies to understand the possible interactions with the active site. **Materials and Methods:** The compounds were synthesized from hippuric acid. The structures of the compounds were confirmed by using spectral (FT-IR, ¹H NMR and Mass) analysis. Cytotoxic potential of the title compounds was determined by using MTT assay, on MCF-7, HeLa and A549 cell lines. **Results:** Marked cytotoxicity was observed for 3,4,5-trimethoxy derivative **3g** (IC₅₀-17.12 μM) towards MCF 7 cell lines, followed by 4-dimethyl amino derivative **3i** (IC₅₀-34.33 μM), while the standard drug Cisplatin exhibited the IC₅₀ value of 12.06 μM. Compounds 3g and 3i also showed significant cytotoxicity in HeLa cell lines. Cytotoxicity results were well correlated with *in vitro* antioxidant activity of the compounds. These compounds also showed good binding interactions towards Estrogen Receptor (ER), Progesterone Receptor (PR) and human epidermal growth factor receptor 2 (HER2). The compounds were also able to comply drug-likeness, passed pharmacokinetic filters and do not have affinity for P-glycoprotein. **Conclusion:** The present study reveals the potential cytotoxicity of 2-mercapto-5-styryl substituted 1,3,4-oxadiazoles.

Keywords: Styryl-1,3,4-oxadiazoles, cytotoxicity, antioxidant activity, estrogen receptor

INTRODUCTION

Oxadiazoles serve as key pharmacophoric elements in medicinally important compounds. 1,3,4-oxadiazoles with different substitutions at 2 and 5 positions are endowed with a wide range of activities such as anti-inflammatory, anticonvulsant, antidepressant, hypoglycemic, antitubercular, antiviral, and anticancer.^[1-5] 1,3,4-oxadiazole ring interacts with a wide variety of pharmacological targets (i) by acting as hydrogen bond acceptor, (ii) by π - π stacking, and (iii) by cation- π interactions.^[6] Diverse substitutions were introduced on 1,3,4-oxadiazole scaffolds to enhance the anticancer activity toward different types of cell lines.^[7,8]

Although numerous studies have been reported on 1,3,4-oxadiazoles, especially styryl bearing 1,3,4-oxadiazoles as potential antitubercular, antimicrobial, antioxidant, and anticholinesterase agents, limited scientific reports are available on 1,3,4-oxadiazoles substituted with styryl moiety as anticancer agents.^[9-11] The presence of thiol group on various

heterocyclics such as triazoles and oxadiazoles was found to enhance various biological activities of these compounds.^[12] Anticancer agents such as 6-mercaptapurine contain thiol group which contributes significantly to the cytotoxicity.

Treatment of various types of cancers is exceptionally challenging with enhanced incidences of resistance and genotoxicity of the existing anticancer agents. Various substituted 1,3,4-oxadiazoles were reported to exhibit anticancer activity by interacting with targets such as epidermal growth factor receptor (EGFR) tyrosine kinase, estrogen receptor (ER), and vascular endothelial growth factor.^[13-15] Zibotentan, an experimental anticancer drug which acts by antagonizing endothelin A receptor possesses 1,3,4-oxadiazole ring in its structure.^[16]

Based on these literature findings, in the present study, 1,3,4-oxadiazole nucleus is coupled with styryl moiety at position five and thiol group at position two. The styryl moiety was further substituted with benzoylamino group

on α -carbon and different substitutions on the phenyl ring. Cytotoxic potential of the synthesized compounds was evaluated using MCF-7, HeLa, and A549 cell lines. The compounds were screened for free radical scavenging potencies using *in vitro* antioxidant assays (2,2-Diphenyl-1-picrylhydrazyl [DPPH], nitric oxide [NO], and 2,2-Azino-bis-3-ethylbenzothiazoline-6-sulfonic acid [ABTS] scavenging assays). The binding orientation and interactions of the title compounds were predicted by molecular docking simulations with ER, progesterone receptors (PR), and human EGFR 2 (HER2), which are associated with breast tumor genesis and invasion. Molecular descriptors and pharmacokinetic parameters were predicted using *in silico* tools to study the drug-likeness and probable affinity of the title compounds toward P-glycoprotein (P-gp). Therapeutic efficacy of drug molecules is severely limited due to the high expression of P-gp in cancerous cells as drugs which serve as P-gp substrates are pumped out of the cells and become ineffective in cancer treatment.^[17]

MATERIALS AND METHODS

Materials

All the chemicals and solvents were procured from Sigma-Aldrich, USA, Merck, HiMedia and SD Fine Chemicals, Mumbai. The reactions were monitored by thin-layer chromatography (TLC) on pre-coated silica gel G TLC sheets. Bruker Fourier-transform infrared (FT-IR) spectrophotometer was used to record IR spectra of the test compounds. Bruker Avance, 400 MHz was used to record ¹H NMR spectral data. Mass spectra were obtained from the apex mass spectrum (300800.D).

Methodology

Synthesis of N-(1-(2-mercapto-1,3,4-oxadiazol-2-yl)-5-substituted phenylvinyl) benzamide (3a-3m)

Step I: Synthesis of 4-benzylidene-2-phenyloxazol-5(4H)-one (1a)

Hippuric acid (0.25 mol) and benzaldehyde (0.25 mol) were mixed in a round bottomed flask. To this mixture acetic anhydride (0.75 mol) and anhydrous sodium acetate (0.25 mol) were added and later was liquefied in a water bath with constant shaking. The reaction mixture was refluxed for 2–2.5 h and after cooling at room temperature, 100 ml of ethanol was slowly added and the solution was kept in a refrigerator overnight. The resulting yellow precipitate (1a) was filtered, washed with 15 ml of hot water and 10 ml of ice cold alcohol, twice successively and later dried at 100°C. The product was recrystallized from ethanol.^[18] Different substituted 4-benzylidene-2-phenyloxazol-5(4H)-ones (1b-1m) were synthesized using substituted aromatic aldehydes by similar methodology.

Step II: Synthesis of N-(3-hydrazinyl-3-oxo-1-phenylprop-1-en-2-yl) benzamide (2a)

Oxazolone (1a) (0.03 mol) was mixed with a solution of hydrazine hydrate (0.06 mol) in ethanol (25 ml) and stirred for 30 min. The solid which was obtained was filtered, washed, and recrystallized from methanol.^[18] Various substituted hydrazides (2b-2m) were synthesized by following the similar procedure.

Step III: Synthesis of N-(1-(5-mercapto-1, 3, 4-oxadiazol-2-yl)-2-phenylvinyl) benzamide (3a)

To a solution of hydrazide (0.1 mol) in ethanol (25 ml), potassium hydroxide (0.1 mol) in absolute ethanol (50 ml) and carbon disulfide (0.2 mol) was added and the contents were refluxed for 5 h. The reaction mixture was cooled and diluted with water. On acidification with dilute hydrochloric acid, the product was precipitated out and was filtered, washed with cold water and recrystallized from ethanol.^[12] Different N-(1-(2-mercapto-1,3,4-oxadiazol-2-yl)-5-substituted phenylvinyl) benzamides (3b-3m) were synthesized in similar manner.

Spectral Data of the Title Compounds

N-(5-(4-phenyl)-1-(2-mercapto-1,3,4-oxadiazol-2-yl) vinyl) benzamide (3a)

mp-100-102°C, yield-30%, FT-IR: (KBr) cm^{-1} : 3162.22, (N-H str of amide), 3090.36 (C-H str, Ar-H), 2911.37 (S-H str), 1672.47 (C=O str), 1488.16 (C=N str of 1,3,4-oxadiazole), 1170.05 (C-O-C str of 1,3,4-oxadiazole); ¹H NMR (CDCl_3 -d₆, 400 MHz) δ (ppm): 6.31 (s, 1H, olefinic), 7.29–7.72 (m, 10H, Ar-H), 8.38 (d, 1H, CONH), 13.87 (s, 1H, SH); MS (EI) m/z: 324 [M+H]⁺ (calculated for C₁₇H₁₃N₃O₂S, 323.37).

N-(5-(4-chlorophenyl)-1-(2-mercapto-1,3,4-oxadiazol-2-yl) vinyl) benzamide (3b)

mp-170–171°C, yield-15%, FT-IR: (KBr) cm^{-1} : 3281.83 (N-H str of amide), 3095.43 (C-H str, Ar-H), 2916.77 (S-H str), 1675.27 (C=O str of amide), 1495.11 (C=N str of 1,3,4-oxadiazole), 1177.01 (C-O-C str of 1,3,4-oxadiazole); ¹H NMR (CDCl_3 -d₆, 400 MHz) δ (ppm): 6.29 (s, 1H, olefinic), 7.27–7.69 (m, 9H, Ar-H), 8.37 (d, 1H, CONH), 13.87 (s, 1H, SH); MS (EI) m/z: 358 [M+H]⁺ (calculated for C₁₇H₁₂ClN₃O₂S, 357.81).

N-(5-(4-methoxyphenyl)-1-(2-mercapto-1,3,4-oxadiazol-2-yl) vinyl) benzamide (3c)

mp-198–200°C, yield-57%, FT-IR: (KBr) cm^{-1} : 3057.51 (N-H str), 2921.42 (C-H str, Ar-H), 2805.80 (S-H str), 1671.31 (C=O str), 1495.13 (C=N str of 1,3,4-oxadiazole), 1176.37 (C-O-C str of 1,3,4-oxadiazole); ¹H NMR (CDCl_3 -d₆, 400 MHz) δ (ppm): 3.34 (s, 3H, OCH₃), 6.09 (s, 1H, olefinic), 6.98–7.71 (m, 9H, Ar-H), 8.49 (d, 1H, CONH), 13.12 (s, 1H, SH); MS (EI) m/z: 353 [M]⁺ (calculated for C₁₈H₁₅N₃O₃S, 353.39).

N-(5-(4-fluorophenyl)-1-(2-mercapto-1,3,4-oxadiazol-2-yl) vinyl) benzamide (3d)

mp-118–120°C, yield-30%, FT-IR: (KBr) cm^{-1} : 3069.64 (N-H str), 2822.40 (C-H str, Ar-H), 2543.96 (S-H str), 1679.00 (C=O str), 1451.91 (C=N str of 1,3,4-oxadiazole), 1177.39 (C-O-C str of 1,3,4-oxadiazole); ¹H NMR (CDCl_3 -d₆, 400 MHz) δ (ppm): 5.02 (s, 1H, olefinic), 6.02–7.19 (m, 9H, Ar-H), 8.98 (d, 1H, CONH), 13.16 (s, 1H, SH); MS (EI) m/z: 341 [M]⁺ (calculated for C₁₇H₁₂FN₃O₂S, 341.36).

N-(5-(4-hydroxy-3-methoxyphenyl)-1(2-mercapto-1,3,4-oxadiazol-2-yl) vinyl) benzamide (3e)

mp-140–150°C, yield-40%, FT-IR: (KBr) cm^{-1} : 3403.95 (N-H str), 3384.69 (O-H str), 2943.30 (C-H str, Ar-H), 2648.83 (S-H str), 1661.30 (C=O str), 1507.19 (C=N str of

1,3,4-oxadiazole), 1149.55 (C-O-C str of 1,3,4-oxadiazole); ¹H NMR (CDCl₃-d₆, 400 MHz) δ (ppm): 3.45 (s, 3H, OCH₃), 6.13 (s, 1H, olefinic), 7.17–7.61 (m, 8H, Ar-H), 9.37 (d, 1H, CONH), 9.87 (s, 1H, OH), 13.09 (s, 1H, SH); MS (EI) m/z: 369.39 [M]⁺ (calculated for C₁₈H₁₅N₃O₄S, 369.39).

N-(5-(4-hydroxy phenyl)-1(2-mercapto-1,3,4-oxadiazol-2-yl) vinyl) benzamide (3f)

mp-195–196°C, yield-45%, FT-IR: (KBr) cm⁻¹: 3408.92 (N-H str), 3388.63 (O-H str), 2943.36 (C-H str, Ar-H), 2646.54 (S-H str), 1661.44 (C=O str), 1509.36 (C=N str of 1,3,4-oxadiazole), 1149.25 (C-O-C str of 1,3,4-oxadiazole); ¹H NMR (CDCl₃-d₆, 400 MHz) δ (ppm): 6.16 (s, 1H, olefinic), 7.20–7.62 (m, 9H, Ar-H), 9.32 (d, 1H, CONH), 9.81 (s, 1H, OH), 13.03 (s, 1H, SH); MS (EI) m/z: 339 [M]⁺ (calculated for C₁₇H₁₃N₃O₃S, 339.37).

N-(1-(2-mercapto-1,3,4-oxadiazol-2-yl)-5-(3,4,5-trimethoxyphenyl) vinyl) benzamide (3g)

mp-136–138°C, yield-20%, FT-IR: (KBr) cm⁻¹: 3342.74 (N-H str), 2840.26 (C-H str, Ar-H), 2737.26 (S-H str), 1674.73 (C=O str), 1509.06 (C=N str of 1,3,4-oxadiazole), 1212.88 (C-O-C str of 1,3,4-oxadiazole); ¹H NMR (CDCl₃-d₆, 400 MHz) δ (ppm): 3.01 (s, 6H, (OCH₃)₂), 3.41 (s, 3H, OCH₃), 6.12 (s, 1H, olefinic), 7.05–7.81 (m, 7H, Ar-H), 9.19 (d, 1H, CONH), 13.24 (s, 1H, SH); MS (EI) m/z: 413 [M]⁺ (calculated for C₂₀H₁₉N₃O₅S, 413.45).

N-(1-(2-mercapto-1,3,4-oxadiazol-2-yl)-5-(*p*-tolyl) vinyl) benzamide (3h)

mp-108–110°C, yield-23%, FT-IR: (KBr) cm⁻¹: 3356.17 (N-H str), 3092.32 (C-H str, Ar-H), 2822.40 (S-H str), 1672.48

(C=O str), 1572.62 (C=N str of 1,3,4-oxadiazole), 1173.33 (C-O-C str of 1,3,4-oxadiazole); ¹H NMR (CDCl₃-d₆, 400 MHz) δ (ppm): 2.81 (s, 3H, CH₃), 6.29 (s, 1H, olefinic), 6.78–7.81 (m, 9H, Ar-H), 9.09 (d, 1H, CONH), 13.22 (s, 1H, SH); MS (EI) m/z: 337 [M]⁺ (calculated for C₁₈H₁₅N₃O₂S, 337.40).

N-(5-(4(dimethylamino) phenyl)-1-(2-mercapto-1,3,4-oxadiazol-2-yl) vinyl) benzamide (3i)

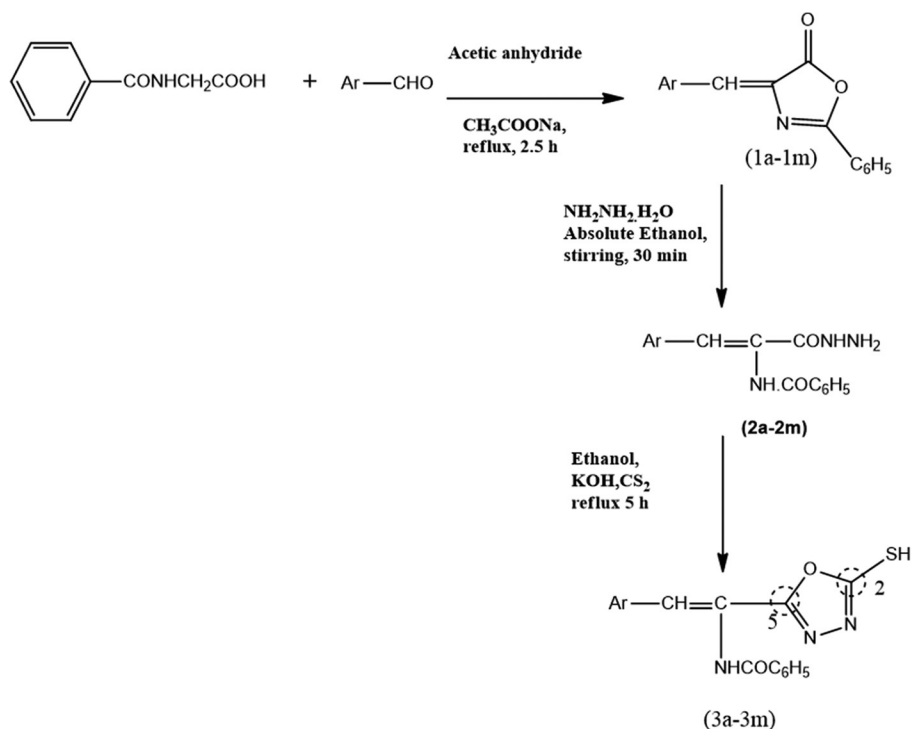
mp-141–142°C, yield-62%, FT-IR: (KBr) cm⁻¹: 3255.47 (N-H str), 2917.18 (C-H str, Ar-H), 2850.11 (S-H str), 1711.05 (C=O str), 1597.79 (C=N str of 1,3,4-oxadiazole), 1103.10 (C-O-C str of 1,3,4-oxadiazole); ¹H NMR (CDCl₃-d₆, 400 MHz) δ (ppm): 3.26 (d, 6H, -N(CH₃)₂), 6.02 (s, 1H, olefinic), 6.47–7.43 (m, 9H, Ar-H), 9.18 (d, 1H, CONH), 13.38 (s, 1H, SH); MS (EI) m/z: 366 [M]⁺ (calculated for C₁₉H₁₈N₄O₂S, 366.44).

N-(1-(2-mercapto-1,3,4-oxadiazol-2-yl)-5-(naphthalen-2-yl) vinyl) benzamide (3j)

mp-125–126°C, yield-56 %, FT-IR: (KBr) cm⁻¹: 3326.64 (N-H str), 3071.76 (C-H str, Ar-H), 2960.14 (S-H str), 1686.14 (C=O str), 1594.69 (C=N str of 1,3,4-oxadiazole), 1259.90 (C-O-C str of 1,3,4-oxadiazole); ¹H NMR (CDCl₃-d₆, 400 MHz) δ (ppm): 6.09 (s, 1H, olefinic), 7.27–8.30 (m, 12H, Ar-H), 9.89 (d, 1H, CONH), 13.42 (s, 1H, SH); MS (EI) m/z: 373 [M]⁺ (calculated for C₂₁H₁₅N₃O₂S, 373.43).

N-(5-(2-hydroxy phenyl)-1(2-mercapto-1,3,4-oxadiazol-2-yl) vinyl) benzamide (3k)

mp-156–158°C, yield-25%, FT-IR: (KBr) cm⁻¹: 3402.90 (N-H str), 3388.68 (O-H str), 2944.36 (C-H str, Ar-H), 2646.62 (S-H str), 1661.46 (C=O str), 1510.34 (C=N str of



Ar= C₆H₅, 4-ClC₆H₄, 4-OCH₃C₆H₄, 4-F C₆H₄, 4-OH C₆H₄, 3,4,5-(OCH₃)₃C₆H₂, 4-CH₃C₆H₄, 4-N(CH₃)₂ C₆H₃, 2-OH C₆H₄, 2-Cl C₆H₄, 2-NO₂ C₆H₄, 1-naphthyl

Scheme 1: Synthesis of 2-mercapto-5-substituted styryl-1,3,4-oxadiazoles (3a-3m)

1,3,4-oxadiazole), 1149.33 (C-O-C str of 1,3,4-oxadiazole); ¹H NMR (CDCl₃-d₆, 400 MHz) δ (ppm): 6.21 (s, 1H, olefinic), 7.22–7.63 (m, 9H, Ar-H), 9.38 (d, 1H, CONH), 9.88 (s, 1H, OH), 13.12 (s, 1H, SH); MS (EI) m/z: 339 [M]⁺ (calculated for C₁₇H₁₃N₃O₃S, 339.37).

N-(5-(2-chlorophenyl)-1-(2-mercapto-1,3,4-oxadiazol-2-yl) vinyl) benzamide (3I)

mp-166–167°C, yield-25%, FT-IR: (KBr) cm⁻¹: 3287.88 (N-H str), 3090.68 (C-H str, Ar-H), 2906.25 (S-H str), 1675.15 (C=O str), 1495.32 (C=N str of 1,3,4-oxadiazole), 1177.11 (C-O-C str of 1,3,4-oxadiazole); ¹H NMR (CDCl₃-d₆, 400 MHz) δ (ppm): 6.33 (s, 1H, olefinic), 7.25–7.68 (m, 9H, Ar-H), 8.30 (d, 1H, CONH), 13.63 (s, 1H, SH); MS (EI) m/z: 359 [M+2H]⁺ (calculated for C₁₇H₁₂ClN₃O₂S, 357.81).

N-(5-(2-nitrophenyl)-1-(2-mercapto-1,3,4-oxadiazol-2-yl) vinyl) benzamide (3M)

mp-130–132°C, yield-30%, FT-IR: (KBr) cm⁻¹: 3281.88 (N-H str), 3095.68 (C-H str, Ar-H), 2916.82 (S-H str), 1675.32 (C=O str), 1495.23 (C=N str of 1,3,4-oxadiazole), 1177.11 (C-O-C str of 1,3,4-oxadiazole); ¹H NMR (CDCl₃-d₆, 400 MHz) δ (ppm): 6.38 (s, 1H, olefinic), 7.22–7.63 (m, 9H, Ar-H), 8.37 (d, 1H, CONH), 13.69 (s, 1H, SH); MS (EI) m/z: 369 [M+H]⁺ (calculated for C₁₇H₁₂N₄O₄S, 368.37).

In vitro Cytotoxicity by 3-(4,5-Dimethylthiazol-2-yl)-2,5-diphenyltetrazolium bromide (MTT) Assay

MTT assay was performed on MCF-7, HeLa, and A549 cell lines with three individual experiments with six concentrations of compounds in triplicates. To identify the viable cells in cell suspension, cells were trypsinized and performed the Trypan blue assay. Haemocytometer was used to count the cells and seeded at a density of 5.0 × 10³ cells/well in 100 μl media in 96 well plate culture medium and incubated overnight at 37°C. The old media were replaced with fresh media (100 μl) with different concentrations of test samples (5, 10, 25, 50, 75, and 100 μM) in 96 well plates. After 48 h, the drug solution was discarded and fresh media were mixed with MTT solution (0.5 mg/mL⁻¹) and were added to each well, and the plates were incubated at 37°C for 3 h. At the end of incubation time, precipitates were formed as a result of the reduction of MTT salt to chromophore formazan crystals by the cells with metabolically active mitochondria. The optical density of solubilized crystals in dimethyl sulfoxide was measured at 570 nm on a microplate reader.^[19] Half-maximal inhibitory concentrations (IC₅₀) values were generated for each cell using origin software (www.originlab.com).

$$\% \text{ Inhibition} = 100 (\text{control-treatment})/\text{control}$$

In Vitro Antioxidant Activity Studies

DPPH free radical scavenging activity

The samples with antioxidant properties reduce the purple color of DPPH free radical to light yellow, because of its tendency to donate protons. In brief, 2 ml sample solutions (at 5, 10, 20, 40, 80, and 100 μM concentrations) were added to 2 ml of 100 μM DPPH solutions. After 20 min of incubation at ambient

temperature, absorbance was determined at 517 nm.^[20] The results were compared using reference compound ascorbic acid. DPPH scavenging activity was calculated using the formula:

$$\% \text{ Scavenging of DPPH} = \frac{\text{Absorbance (control-test)}}{\text{absorbance of control}} \times 100$$

IC₅₀ were determined using a plot of absorbance and % scavenging activity.

NO scavenging assay

All the synthesized compounds were screened for NO scavenging activity. The methanolic solutions (2 ml) of the sample (at 5, 10, 20, 40, 80, and 100 μM concentrations) were mixed with sodium nitroprusside (5 mM) in standard phosphate buffer (pH 7.4). After the incubation at 25°C for 5 h, 2 ml of sample solutions were diluted with 2 ml of Griess reagent and absorbance was measured at 546 nm.^[21] Ascorbic acid was used as the standard in this assay. % NO scavenging activity was calculated using the given equation and IC₅₀ was determined.

$$\% \text{ Scavenging activity} = \frac{\text{Absorbance (control-test)}}{\text{absorbance of control}} \times 100$$

ABTS diammonium salt scavenging assay

ABTS assay measures the relative ability of antioxidants to scavenge the ABTS free radical generated from the reaction between ABTS and a strong oxidizing agent such as potassium persulfate.^[22] The assay procedure involves the addition of 1 ml of ethanolic solutions of the test compounds (at 5, 10, 20, 40, 80, and 100 μM concentrations) to 1 ml of ABTS solution and the estimation of absorbance at 734 nm. Butylated hydroxytoluene (BHT) was used to compare the results of the ABTS assay. The antioxidant activity was calculated using the formula:

$$\% \text{ Scavenging activity} = \frac{\text{Absorbance (control-test)}}{\text{absorbance of control}} \times 100$$

IC₅₀ was determined using a plot of absorbance and % scavenging activity.

In Silico Studies

Prediction of drug-likeness and pharmacokinetic parameters

Molinspiration, on-line tool (<http://www.molinspiration.com>), was used for the computation of molecular descriptors such as Log P, topological surface area, molecular volume, number of hydrogen bond donors, and acceptors. Bioactivity scores for ion channel modulators, nuclear receptor ligand, protease inhibition, kinase inhibition, enzyme inhibition, and G-protein coupled receptor (GPCR) ligand were also calculated by molinspiration tool. Swiss ADME (<http://www.swissadme.ch>), was applied to predict ADME parameters such as gastrointestinal (GI) absorption, blood-brain barrier penetration, affinity toward P-gp and bioavailability.

Molecular docking studies

The synthesized compounds were subjected to molecular docking studies using Swiss Dock (<http://www.swissdock.ch>), and their probable binding modes and the interactions were

predicted. Target receptor structures (ER, protein data bank [PDB] ID: 3ERT; PR, PDB ID: 1SQN; HER2, PDB ID: 1N8Z) were retrieved from the PDB (www.rcsb.org). Chem and Bio 3D 12.0 was applied to draw the chemical structures of the title compounds and saved in mol2 format. Whole protein structure, i.e., total surface, was selected, and blind docking mode was applied. Docking was continued with the default setting provided by Swiss Dock server. Swiss Dock generates the results as favorable clusters formed by EADock DSS algorithm.^[23] Preferred binding modes were visualized using discovery studio visualizer 2019. To validate the docking protocol, in-built ligands from the cocrystallized structure of proteins retrieved from the PDB were used.

RESULTS AND DISCUSSION

Chemistry

N-(1-(2-mercapto-1,3,4-oxadiazol-2-yl)-5-substituted phenylvinyl) benzamides (**3a-3m**) were synthesized by the following steps: At first, substituted oxazolones (**1a-1m**) were prepared by the condensation between hippuric acid and substituted benzaldehyde in the presence of acetic anhydride and sodium acetate. The resulting oxazolones were converted to the corresponding hydrazides (**2a-2m**) by stirring with hydrazine hydrate in ethanol. Finally, the title compounds (**3a-3m**) were synthesized by refluxing the substituted hydrazides (**2a-2m**) in ethanol, potassium hydroxide, and carbon disulfide. IR spectra showed a strong amide N-H stretching band around 3255 cm^{-1} and S-H stretching band around 2916 cm^{-1} . The absorption band around 1495 cm^{-1} evidenced the presence of C=N stretching of 1,3,4-oxadiazoles. ^1H NMR spectra displayed peaks at δ (ppm) values of 2.81, 3.34, and 9.87, indicating the presence of methyl, methoxy, and hydroxyl protons, respectively, in the compounds. The multiplets in the region of δ 6.78–7.81 showed the presence of aromatic protons. δ values around 9.00 indicate the presence of amide protons and SH protons were observed at around 13.5.

In Vitro Cytotoxicity by MTT Assay

MCF-7, HeLa, and A 549 cell lines were used to evaluate the *in vitro* cytotoxicity, and the results were compared using cisplatin as standard. Among the tested compounds, 3g (3,4,5-trimethoxy phenyl) showed promising cytotoxicity against MCF-7 cell lines with IC_{50} value of 17.12 μM , while cisplatin showed IC_{50} value of 12.06 μM . 4-Dimethylamino phenyl derivative (3i) exhibited good cytotoxicity with IC_{50} value of 34.33 μM , while the compounds substituted with 4-hydroxy, 4-methoxy and 4-methyl groups showed moderate cytotoxicity ($\text{IC}_{50} > 68 \mu\text{M}$). The remaining compounds displayed poor cytotoxicity.

The title compounds were designed involving structural variation on the phenyl ring of styryl moiety by introducing various substitutions with electron donating and withdrawing properties, increase in size and polarity, etc. The marked difference in the inhibitory effect of compounds on malignant cells clearly suggested the crucial role of substituent groups on the phenyl ring of styryl moiety. 3,4,5-Trimethoxy and 4-dimethyl amino groups are the most favorable for cytotoxicity. Substitution by other electron-donating groups such as 4-hydroxy, 4-methoxy, and 4-methyl

enhanced the cytotoxicity. Interestingly, when the phenyl ring is replaced with naphthyl moiety activity was retained.

Various substitutions or aryl/heteroaryl rings were introduced at second and fifth positions of oxadiazole ring explore the cytotoxic effects of 1,3,4-oxadiazoles in the previous studies.^[24-27] Although it is difficult to mention inclusive structure activity relationships, many studies have highlighted the importance of electron-donating groups such as hydroxy and methoxy groups for good cytotoxicity against various cell lines. A number of naturally occurring antitumor agents such as podophyllotoxin, colchicine, and combretastatin possess 3,4,5-trimethoxy phenyl ring in their structures, which plays a key role in binding of these drugs at the target active site.^[28,29] Interestingly, compound 3g displayed promising cytotoxicity with IC_{50} of 17.12 μM , almost comparable to cisplatin. Literature revealed that 3,4,5-trimethoxy phenyl group is considered as a potent fragment which occupies favorable region in the colchicine binding site.^[30] These results suggested the importance of 3,4,5-trimethoxy phenyl substitution in imparting the cytotoxicity of the molecules against MCF-7 cell lines.

Thiol group is a potent free radical scavenger with the ability to conjugate metals. Reactive oxygen species play a crucial role in cell proliferation and tumor growth and a free radical scavenger can inhibit cell growth by trapping free radicals. The collective contribution of thiol group, 3,4,5-trimethoxy phenyl, benzoyl amino moieties, and 1,3,4-oxadiazole nucleus toward the significant cytotoxicity of the compound (3g) was observed in our findings. Benzoylamino group also possesses the ability to establish hydrogen bonding and π - π stacking interactions.^[31] Electron donating and steric features profoundly influenced the cytotoxicity of the test compounds.

Compounds 3g and 3i, which showed appreciable activity against MCF-7 cell lines, were evaluated further against HeLa and A549 cell lines. These derivatives showed IC_{50} values of 61.67 and 43.30 μM and 193.73 and 29.07 μM , respectively (Cisplatin, IC_{50} values of 5.59 μM for HeLa and 4.96 μM for A549). Compounds 3g and 3i exhibited cytotoxicity in both the cell lines, but greater selectivity was seen in the case of breast cancer cell lines [Table 1].

In Vitro Antioxidant Activities

The results of *in vitro* antioxidant assays are given in Table 1. Vanillyl derivative (3e) showed the highest antioxidant activity (in scavenging the DPPH free radicals) with IC_{50} value of 26.5 μM , followed by 4-methoxy phenyl (3c) and 4-methyl phenyl (3h) derivatives (IC_{50} , 35.44 and 45.41 μM). These derivatives displayed better antioxidant activity than ascorbic acid, with IC_{50} value of 45.50 μM . The results showed the importance of electron-donating groups such as hydroxyl, methoxy, and methyl groups on the phenyl ring and, however, 4-dimethylamino (3i) and 2-hydroxy (3k) derivatives also displayed good antioxidant activity. Derivatives containing electron-withdrawing groups (3b, 3d, 3l, and 3m) displayed poor antioxidant activity.

The results of NO scavenging assay indicated that 3g (3,4,5-trimethoxy phenyl) displayed promising activity with IC_{50} value of 36.99 μM . This result is correlated with the marked cytotoxicity of this derivative against MCF-7 cell lines. Compounds 3c and 3h also displayed good antioxidant activity with IC_{50} values of 48.30 and 52.36 μM , respectively. These

two compounds displayed improved NO scavenging activity when compared to the standard ascorbic acid (58.71 μM).

The results obtained from ABTS assay highlighted the compound 3c, which exhibited marked antioxidant activity with IC_{50} value of 28.57 μM , better than the standard drug BHT (IC_{50} , 32.69 μM). This compound also displayed good DPPH radical scavenging activity. Compounds 3e and 3h showed good ABTS scavenging activity with IC_{50} values of

37.4 and 38.06 μM , respectively. The results obtained from the *in vitro* antioxidant studies revealed the importance of electron releasing groups, in exhibiting significant antioxidant activity.

The findings observed from *in vitro* antioxidant studies support the significant cytotoxicity of compounds 3c, 3h, 3i, and 3g which might be partly due to their radical scavenging ability.

Table 1: Anticancer and antioxidant activity of title compounds (3a-3m)

Compound	Ar	Anticancer activity			Antioxidant activity ^b		
		MCF-7 IC_{50} (μM)	HeLa ^a IC_{50} (μM)	A549 ^a IC_{50} (μM)	DPPH scavenging activity IC_{50} (μM)	Nitric oxide scavenging activity IC_{50} (μM)	ABTS scavenging activity IC_{50} (μM)
3a	C ₆ H ₅	85.52	-	-	128.89±3.2	214.36±2.0	64.07±5.1
3b	4-ClC ₆ H ₄	118.52	-	-	180.07±3.5	100.19±2.72	133.59±7.1
3c	4-OCH ₃ C ₆ H ₄	63.86	-	-	35.44±3.1	48.30±4.2	28.57±5.1
3d	4-F C ₆ H ₄	121.25	-	-	166.54±4.3	467.85±4.4	96.71±2.2
3e	4-OH,3-OCH ₃ C ₆ H ₃	1459.16	-	-	26.5±2.3	546.76±5.4	38.06±1.2
3f	4-OH C ₆ H ₄	61.76	-	-	86.81±3.1	254.71±5.25	63.33±2.5
3g	3,4,5-(OCH ₃) ₃ C ₆ H ₂	17.12	61.67	193.73	85.18±5.1	36.99±3.3	79.02±1.8
3h	4-CH ₃ C ₆ H ₄	67.33	-	-	45.41±0.9	52.36±5.2	37.4±1.8
3i	4-N(CH ₃) ₂ C ₆ H ₃	34.33	43.30	29.07	50.05±4.7	97.76±4.5	46.23±1.8
3j	1-naphthyl	82.63	-	-	426.5±3.5	239.33±6.1	164.5±3.4
3k	2-OH C ₆ H ₄	NT	-	-	57.80±4.9	96.20±3.8	56.71±1.2
3l	2-Cl C ₆ H ₄	137.05	-	-	134.90±4.6	273.25±10.1	-
3m	2-NO ₂ C ₆ H ₄	NT	-	-	648.88±5.9	71.45±2.8	-
Standard		12.06 (cisplatin)	5.59 (cisplatin)	4.96 (cisplatin)	45.50±2 (ascorbic acid)	58.71±2.5 (ascorbic acid)	32.69±2.0 (butylated hydroxy toluene)

NT: Not tested, ^aselected active compounds were tested against HeLa and A549 cell lines, ^bvalues are mean±standard deviation of three replicates.
ABTS: 2,2-Azino-bis-3-ethylbenzothiazoline-6-sulfonic acid, DPPH: 2,2-Diphenyl-1-picrylhydrazyl

Table 2: Predicted molecular properties of the title compounds (3a-3m)

Compound	mLog P	TPSA	MW	N.ON	NOHNH	N.ROT	Lipinski rule
3a	2.83	68.02	323.38	5	1	4	Yes
3b	3.50	68.02	357.82	5	1	4	Yes
3c	2.88	77.26	353.40	6	1	5	Yes
3d	2.99	68.02	341.37	5	1	4	Yes
3e	2.17	97.48	369.40	7	2	5	Yes
3f	2.35	88.25	339.38	6	2	4	Yes
3g	2.46	95.72	413.45	8	1	7	Yes
3h	3.27	68.02	337.40	5	1	4	Yes
3i	2.63	71.26	380.47	6	1	6	Yes
3j	3.81	68.02	373.44	5	1	4	Yes
3k	2.59	88.25	339.38	6	2	4	Yes
3l	3.28	68.02	357.82	5	1	4	Yes
3m	2.56	113.85	368.37	8	1	5	Yes

mLog P: Logarithm of partition coefficient between n-octanol and water, TPSA: Topological polar surface area, N.ON: Number of hydrogen bond acceptors, N.OHNH: Number of hydrogen bond donors, N.ROT: Number of rotatable bonds, MW: Molecular weight

Table 3: Bioactivity scores of the title compounds (**3a-3m**)

Compound	G-protein coupled receptor ligand	Kinase inhibitor	Protease inhibitor	Enzyme inhibitor
3a	-0.48	-0.27	-0.26	-0.23
3b	-0.45	-0.28	-0.27	-0.26
3c	-0.48	-0.29	-0.27	-0.26
3d	-0.44	-0.23	-0.25	-0.24
3e	-0.44	-0.24	-0.29	-0.21
3f	-0.41	-0.22	-0.21	-0.17
3g	-0.44	-0.25	-0.28	-0.23
3h	-0.50	-0.30	-0.29	-0.28
3i	-0.31	-0.14	-0.12	-0.16
3j	-0.35	-0.17	-0.12	-0.14
3k	-0.45	-0.25	-0.23	-0.20
3l	-0.48	-0.39	-0.29	-0.30
3m	-0.57	-0.44	-0.44	-0.37

Table 4: Drug-likeness properties of the title compounds

Compound	Bioavailability	BBB permeant	P-gp substrate	Drug likeness and BS
3a	High	No	No	Yes (0.55)
3b	High	No	No	Yes (0.55)
3c	High	No	No	Yes (0.55)
3d	High	No	No	Yes (0.55)
3e	High	No	No	Yes (0.55)
3f	High	No	No	Yes (0.55)
3g	Low	Low	No	Yes (0.55)
3h	High	No	No	Yes (0.55)
3i	High	No	No	Yes (0.55)
3j	High	No	No	Yes (0.55)
3k	High	No	No	Yes (0.55)
3l	High	No	No	Yes (0.55)
3m	Low	No	No	Yes (0.55)

BBB: Blood-brain barrier, P-gp: Permeability glycoprotein, BS: Bioavailability score

In Silico Studies

Prediction of drug-likeness and pharmacokinetic parameters

There is a strong correlation between the oral bioavailability and molecular properties of a drug candidate.^[32,33] All the compounds obeyed the Lipinski rule; Log P values lied in the range of 2.17–3.81; molecular weight: 323.38–413.45; HBD values 1–2; HBA values 5–8, indicating that the properties of the synthesized compounds favor oral bioavailability. All the synthesized compounds (**3a-3m**) showed bioactivity scores ranging from -0.15 to 0.50 (0.00: High activity; -0.50 to 0.00: Moderate activity; ≥ 0.50 : Poor activity), suggesting that the compounds interact moderately with GPCR ligands, kinases, proteases, and enzymes.

Results of Swiss ADME studies indicated that the compounds have shown good GI absorption with few exceptions (3g, 3e, and 3m). The synthesized compounds

do not possess an affinity for P-gp which prevents the cell internalization of chemotherapeutic agents and by being P-gp non-substrates, the compounds will not be extruded out of the cells by efflux transporters.^[34] These *in silico* predictions demonstrated favorable molecular properties of the synthesized compounds. The results are illustrated in Tables 2-4.

Molecular docking studies

Molecular docking studies were performed to study the molecular level interactions of the synthesized compounds. ER, PR, and HER-2 receptors were selected for the studies, which are associated with breast, cervical, and lung cancers. From the cocrystallized structure of protein available in PDB, the ligand was extracted and the docking studies were performed to validate the docking protocol. The best pose was selected based on the binding energy. The docked pose of the ligand was compared with that of cocrystallized structure in terms

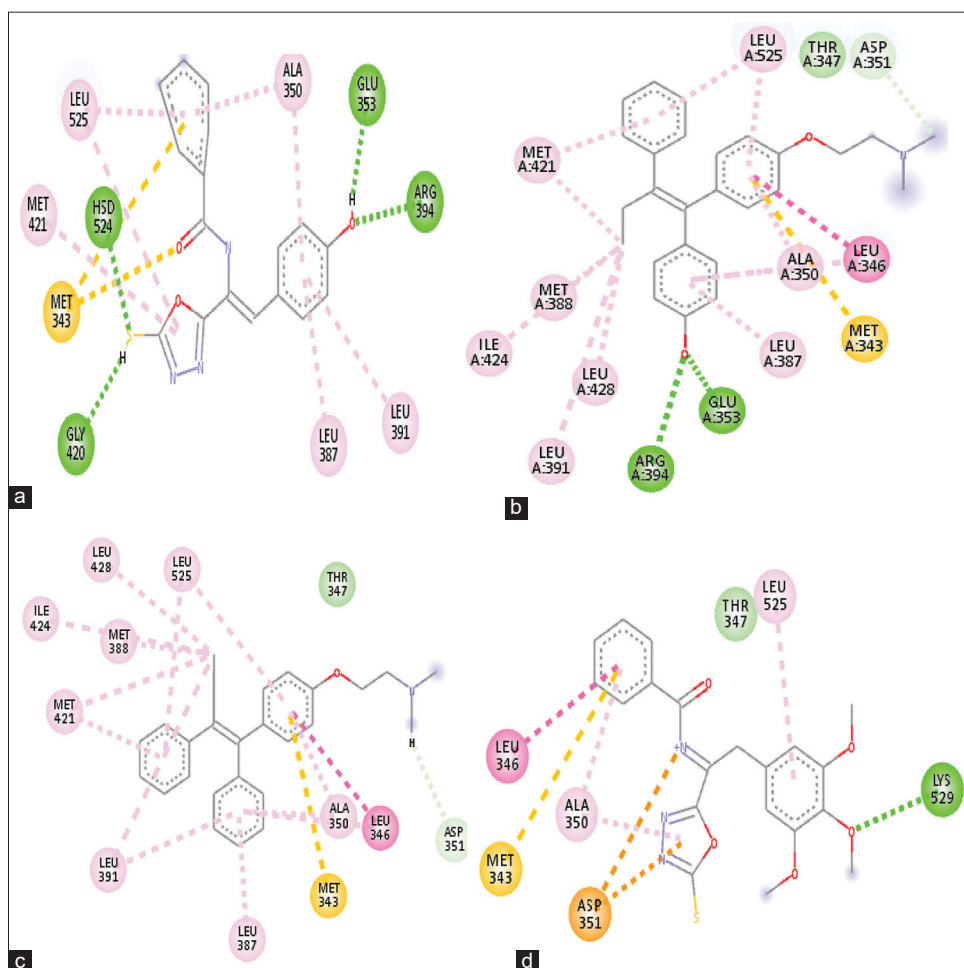
Table 5: Docking scores and interactions of the title compounds with ER (PDB ID: 3ERT)

Compound	Full fitness	ΔG (kcal/mol)	Interacting amino acids	Type of interaction
3a	-1114.56	-9.06	GLU 353, ARG 394	Hydrogen bond
			ALA 350, LEU 387, LEU 391, MET 388, MET 421, LEU 525	Pi-Alkyl
			MET 343	Pi-sulfur
3b	-1104.20	-9.15	LEU 346	Amide-Pi stacked
			GLU 521 HSD 524	Hydrogen bond
			MET 343	Pi-sulfur
3c	-1101.99	-9.27	LEU 346	Amide-Pi stacked
			ALA 350, LEU 384, LEU 387, LEU 391, LEU 525	Pi-alkyl
			MET 343	Pi-sulfur
3d	-1111.47	-9.26	LEU 346	Amide-Pi stacked
			GLU 353, ARG 394, HSD 524	Hydrogen bond
			MET 343	Pi-sulfur
3e	-1097.13	-9.49	ALA 350, LEU 387, LEU 391, LEU 525, ILE 524, MET 421, MET 388	Pi-alkyl
			THR 347, GLU 353	Hydrogen bond
			MET 343	Pi-sulfur
3f	-1107.38	-9.65	LEU 346	Amide-Pi stacked
			GLU 353, ARG394, GLY 420, HSD 524	Hydrogen bond
			MET 343	Pi-sulfur
3g	-1076.55	-8.41	ALA 350, LEU 387, LEU 391, MET 421, LEU 525	Pi-alkyl
			LYS 529	Hydrogen bond
			MET 343	Pi-sulfur
3h	-1103.54	-9.21	ASP 351	Pi-anion
			GLY 521, HSD 524	Hydrogen bond
			LEU 384, LEU 387, LEU 391, LEU 525, ALA 350	Pi-alkyl
3i	-1105.65	-9.14	MET 343	Pi-sulfur
			LEU 346	Amide-Pi stacked
			GLY 521, HSD 524	Hydrogen bond
3j	-1090.03	-9.07	ALA 350, LEU 384, LEU 387, LEU 391, LEU 525	Pi-alkyl
			MET 343	Pi-sulfur
			THR 347	Van der Waals
3k	-1102.50	-9.02	GLY 521, HSD 524	Hydrogen bond
			ALA 350, LEU 387, LEU 391, LEU 384, LEU 525	Pi-alkyl
			MET 343	Pi-sulfur
			ASP 351	Pi-anion
			LEU 346	Amide-Pi stacked
			GLY 41	Hydrogen bond
			PRO 41, PRO 174	Pi-alkyl
			GLY 41	Van der Waals

(Contd...)

Table 5: (Continued)

Compound	Full fitness	ΔG (kcal/mol)	Interacting amino acids	Type of interaction
3l	-1103.94	-9.12	TRP 47, PHE 98 TRP 47	Hydrogen bond Pi-sulfur
3m	-1091.60	-9.07	TYR 95, LEU 115 VAL 93, PRO 156 THR 114	Hydrogen bond Pi-alkyl Van der Waals
4-Hydroxy tamoxifen (In-built ligand)	-1113.60	-10.26	GLU 353, ARG 394 MET 343 ALA 350, LEU 387, MET 388, LEU 491, ILE 424, MET 421, LEU 428, LEU 525	Hydrogen bond Pi-sulfur Pi-alkyl
Tamoxifen (standard)	-2058.66	-8.98	MET 343 LEU 346 ALA 350, LEU 387, LEU 391, LEU 428, LEU 525, ILE 424, MET 388, MET 421 ASP 351	Pi-sulfur Amide-Pi stacked Pi-alkyl Amide-Pi stacked

**Figure 1:** Preferred binding modes of (a) compound 3f (b) compound 3g (c) crystal inhibitor (d) standard inhibitor with the active sites of estrogen receptor in two-dimensional representation

of ligand-receptor interactions and the active site residues. Similar binding modes were reproduced with root-mean

square deviation up to 2.5 Å, which signified the validation of the docking protocol.

Table 6: Docking scores and interactions of the title compounds with PR (PDB ID: 1SQN)

Compound	Full fitness	ΔG (kcal/mol)	Interacting amino acids	Type of interaction			
3a	-2206.58	-9.29	ASN 719, CYS 891	Hydrogen bond			
			LEU 721, MET 759, LEU 763, LEU 797	Pi-alkyl			
			PHE 605, MET 756, CYS 891	Pi-sulfur			
			PHE 778	Amide-Pi stacked			
3b	-2184.68	-7.91	SER 898	Hydrogen bond			
			ARG 899	Pi-anion			
			PHE 895	Van der Waals			
			SER 910	Amide-Pi stacked			
3c	-2198.45	-8.00	ALA 914	Pi-alkyl			
			VAL 730, LYS 734, ILE 748	Pi-alkyl			
			3d	-2203.60	-9.25	ARG 766, CYS 891	Hydrogen bond
						MET 756, CYS 891, PHE 905	Pi-sulfur
3e	-2186.95	-9.10	LEU 721, LEU 791	Pi-Alkyl			
			PHE 778	Amide-Pi stacked			
			MET 759, ARG 766	Hydrogen bond			
			PHE 778	Amide-Pi stacked			
3f	-2212.79	-9.30	LEU 721, MET 759, LEU 763	Pi-alkyl			
			MET 759, ARG 766, CYS 891	Hydrogen bond			
			MET 756, CYS 891, PHE 905	Pi-sulfur			
			LEU 721, LEU 797	Pi-alkyl			
3g	-2168.59	-8.94	PHE 778	Amide-Pi stacked			
			MET 908	Hydrogen bond			
			LEU 726, LEU 727, VAL 730	Pi-alkyl			
			ILE 748	Van der Waals			
3h	-2195.40	-8.94	PHE 905	Van der Waals			
			ALA 914	Pi-alkyl			
3i	-2199.50	-8.03	MET 759, ARG 766	Hydrogen bond			
			LEU 715, LEU 718, MET 756, MET 759	Pi-alkyl			
			ILE 748	Van der Waals			
3j	-2188.59	-8.17	MET 759, ARG 766	Hydrogen bond			
			LEU 721, MET 759, LEU 763	Pi-alkyl			
			PHE 778	Amide-Pi stacked			
3k	-2202.94	-9.03	ASN 719, CYS 891	Hydrogen bond			
			MET 756, PHE 778, LEU 715	Pi-alkyl			
			PHE 905	Van der Waals			
3l	-2193.37	-9.40	ASN 719, CYS 891	Hydrogen bond			
			PHE 705, MET 756, CYS 891	Pi-sulfur			
			LEU 721, MET 759, LEU 763, LEU 797	Pi-alkyl			
3m	-2180.83	-8.73	ASN 719, CYS 891	Hydrogen bond			
			MET 756, PHE 778, LEU 715	Pi-alkyl			
			PHE 905	Van der Waals			
(In-built ligand)	-2238.38	-9.63	ARG 766, ASN 719	Hydrogen bond			
Norethisterone (standard)	-2237.51	-9.60	LEU 715, LEU 718, MET 756, MET 759, TYR 890, CYS 891, PHE 905	Pi-alkyl			
			GLN 725, ARG 766	Hydrogen bond			
			MET 756, PHE 778, LEU 715, LEU 719, LEU 797, LEU 887, MET 759, TYR 890	Pi-alkyl			
			CYS 891	Van der Waals			

Table 7: Docking scores and interactions of the title compounds with HER2 (PDB ID: 1N8Z)

Compound	Full fitness	ΔG (kcal/mol)	Interacting amino acids	Type of interaction
3a	-1762.16	-8.50	TRP 47, PHE 98	Hydrogen bond
			TRP 97	Pi-alkyl
3b	-1765.37	-8.21	TRP 47, PHE 98	Hydrogen bond
			TRP 47, THR 97	Van der Waals
			LYS 43	Pi-alkyl
			TRP 47	Pi-sulfur
3c	-1750.38	-8.70	GLY 42, THR 85, TYR 87	Hydrogen bond
			VAL 93	Pi-alkyl
			LYS 43	Van der Waals
3d	-1757.82	-8.22	TRP 47, PHE 98	Hydrogen bond
			TRP 47	Pi-sulfur
			THR 97	Van der Waals
3e	-1756.97	-8.30	GLN 166	Hydrogen bond
			PRO 40	Van der Waals
			PRO 40, PRO 174	Pi-alkyl
3f	-1770.81	-8.46	GLY 41	Hydrogen bond
			GLY 41	Amide-Pi stacked
			VAL 93, PRO 174	Pi-Alkyl
3g	-1730.79	-8.49	GLY 42	Hydrogen bond
			PRO 41, GLN 112, GLY 113	Van der Waals
			VAL 93	Pi-alkyl
3h	-1760.84	-8.44	GLY 41, GLY 42	Hydrogen bond
			PRO 41, VAL 93	Pi-alkyl
3i	-1762.22	-8.41	TRP 47, PHE 98	Hydrogen bond
			TRP 47	Pi-sulfur
			ALA 61, PRO 95, PRO 96, THR 97	Van der Waals
3j	-1744.53	-8.24	GLY 41	Hydrogen bond
			VAL 93, PRO 174	Pi-alkyl
			TYR 87	Pi-sulfur
3k	-1760.02	-8.40	GLY 41	Hydrogen bond
			PRO 41, PRO 174	Pi-alkyl
			GLY 41	Van der Waals
3l	-1752.93	-8.72	TRP 47, PHE 98	Hydrogen bond
			TRP 47	Pi-sulfur
3m	-1745.23	-8.30	TYR 95, LEU 115	Hydrogen bond
			VAL 93, PRO 156	Pi-alkyl
			THR 114	Van der Waals
Lapatinib (standard inhibitor)	-1793.44	-9.66	GLY 41, THR 85, TYR 87, GLU 155, THR 172, ALA 175	Hydrogen bond
			VAL 93, PRO 174	Pi-alkyl
			GLN 39, HSE 171	Van der Waals
Afitinib (standard inhibitor)	-1789.11	-9.29	THR 85, TYR 87, TYR 95	Hydrogen bond
			GLN 38, GLN 100, GLY 101	Van der Waals
			PRO 40, PRO 41, VAL 93	Pi-alkyl

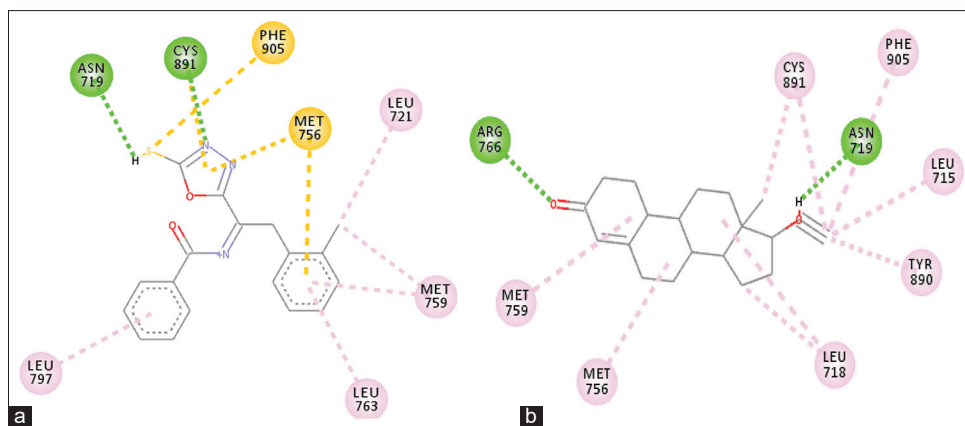


Figure 2: Preferred binding modes of (a) compound 31 (b) crystal inhibitors with the active sites of progesterone receptors in two-dimensional representation

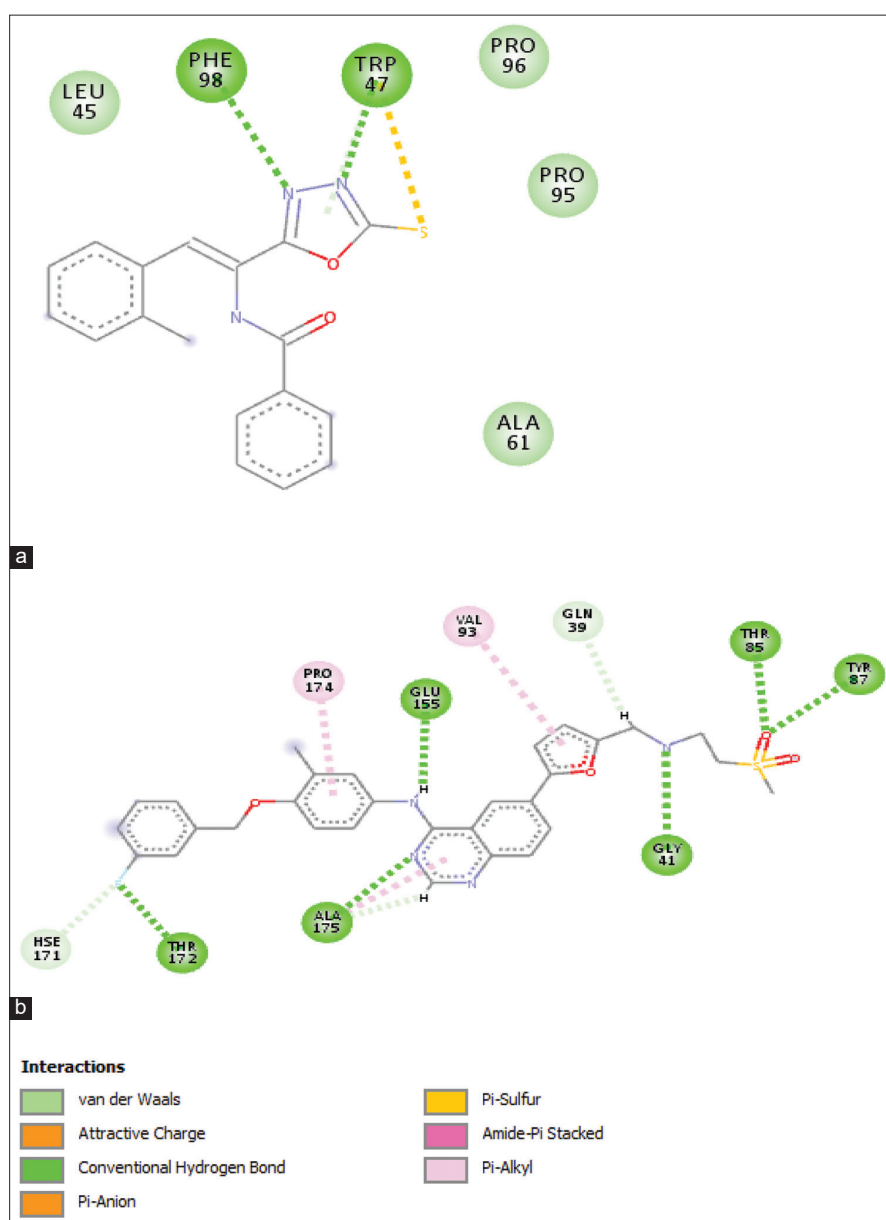


Figure 3: Preferred binding modes of (a) compound 31 (b) lapatinib in the active site of human epidermal growth factor receptor 2 in two-dimensional representation

Molecular Docking Studies with Hormone Receptors ER (PDB ID: 3ERT) and PR (PDB ID: 1SQN)

ER type α is found to be present in 80% of cells and over expressed in epithelial cells of breast tissue. Progesterone, a steroidal hormone plays a key role in the development of mammary carcinoma. Breast adenocarcinoma cells contain either ER or PR or both. In breast cancer, hormone sensitive cells will be protected from hormone stimulation by antagonizing PR in cancer cells.^[35,36] Molecular docking studies were performed to predict the binding affinity of the synthesized compounds toward ER and PR.

The synthesized compounds exhibited moderate to good binding affinity toward ER (ΔG values: -8.82 – -9.65 kcal/mol). The standard inhibitor, tamoxifen showed noticeable binding affinity with ΔG value of 8.98 kcal/mol and in-built ligand, 4-hydroxy tamoxifen exhibited highest affinity with ΔG of -10.26 kcal/mol. Appreciable binding affinity was observed for 3f (4-hydroxy phenyl derivative) (ΔG , -9.65 kcal/mol), whereas the remaining derivatives displayed moderate to weak binding affinities (-8.82 – -9.49 kcal/mol). Figure 1a and b illustrates the preferred binding modes of 3f and 4-hydroxy tamoxifen involving similar binding interactions: (i) Hydrogen bonding with GLY 420, HSD 52, ARG 394, and GLU 353, (ii) π -sulfur interactions with MET 343, and (iii) π -alkyl interactions with ALA 350, LEU 387, LEU-391, LEU 525, and MET 421; 4-hydroxy group of 3f was positioned similar to that of 4-hydroxy group of in-built ligand and interacted with ARG 394 and GLU353, while in case of tamoxifen, these important H-bonds were absent [Figure 1c].

Compound 3g, which displayed potent cytotoxicity against MCF-7 cell lines showed moderate affinity (ΔG , -8.41 kcal/mol) toward ER and interacted with MET 343 (π -sulfur), ASP351 (π -anion), and LEU 346 (amide- π stacked) [Figure 1d]. The decreased affinity of 3g might be due to steric hindrance imposed by trimethoxy group in the binding region and its inability to establish hydrogen bonds with crucial amino acids. Docking scores and interactions toward ER and PR are illustrated in Tables 5 and 6.

Results of molecular docking studies with PR indicated that the title compounds have appreciable binding affinity toward this receptor as shown by ΔG values, ranging from -7.91 kcal/mol to -9.40 kcal/mol and the highest interactive derivative was 3l (2-chlorophenyl). Similar interactions were observed for 3l and in-built ligand [Figure 2a and b]. Compounds 3d, 3e, 3f, 3g, and 3l showed good binding affinities with both these hormone receptors (ER and PR).

Molecular Docking with HER2 (PDB ID: 1N8Z)

Abnormal HER2 gene expression exhibits characteristic uncontrolled cell division and cell growth. HER2 protein is present in high levels at about 30% of breast cancer cells and is also associated with metastasis.^[37] Afatinib and lapatinib were used as standard inhibitors to compare the results obtained [Table 7].

The results revealed that the compounds, 3l and 3c displayed significant binding affinities ($\Delta G = -8.72$ and

-8.70 kcal/mol). Figure 3a and b illustrates the binding poses of 3l and 3c, which established hydrogen bonding interactions (nitrogen of 1,3,4-oxadiazole with PHE 98, TRP 47) and π -sulfur interactions (sulfur of 1,3,4-oxadiazole ring with TRP 47). The standard inhibitors, afatinib and lapatinib displayed significant binding affinity with ΔG values of -9.29 and -9.66 kcal/mol, respectively. Lapatinib participated in three different types of binding interactions with various amino acid residues: (i) Hydrogen bonds with GLY 41, TYR 87, THR 85, THR 172, GLU 155, and ALA 175, (ii) π -alkyl interactions with VAL 93 and PRO 174, and (iii) Van der Waals interactions with GLN 39 and HSE 171.

Compound 3g, that exhibited potent cytotoxicity against MCF-7 cell lines, showed moderate binding affinity (ΔG value of -8.49 kcal/mol) involving hydrogen bonding, π -alkyl and Van der Waals interactions similar to lapatinib [Figure 3b].

1,3,4-Oxadiazoles substituted with mercapto group at second position were found to be contributed for binding with target receptors by establishing π -sulfur, π -alkyl and hydrogen bonding interactions. The presence of benzoylamino and styryl moieties further stabilized the complex by means of π -alkyl interactions.

CONCLUSION

In the present study, a series of substituted 1,3,4-oxadiazoles (**3a-3m**) was synthesized by introducing a thiol group at second position and substituted styryl moiety at fifth position. Additionally benzoylamino group was incorporated on α -carbon of styryl moiety. Results of the cytotoxicity studies against MCF-7, HeLa, and A549 cell lines revealed that 3g (3,4,5-trimethoxy phenyl analog) exhibited potent cytotoxicity. The cytotoxicity of 3g was discernible with IC_{50} of $17.12 \mu M$, against MCF-7 cell lines which is almost comparable to the standard anticancer agent cisplatin (IC_{50} $12.06 \mu M$). The contribution of substituents on styryl moiety for cytotoxicity was well supported by *in vitro* antioxidant and molecular docking studies. Our findings postulate that introduction of a free thiol group at second position and substituted styryl group at fifth position seems to ameliorate the potentiality of 1,3,4-oxadiazole nucleus toward cytotoxicity. Further studies may be needed to explore the detailed mechanisms of 1,3,4-oxadiazoles for the development of better analogs.

REFERENCES

1. Preeti K, Dinesh M, Girish KG, Das R, Kaur K. A brief review on oxadiazole as a potent anticancer agent. *Inventi Rapid* 2013;4:1-9.
2. Azam MA, Suresh B, Kalsi SS, Antony AS. Synthesis and biological evaluation of some novel 2-mercaptobenzothiazoles carrying 1, 3, 4-oxadiazole, 1,3,4-thiadiazole and 1,2,4-triazole moieties. *S Afr J Chem* 2010;63:114-22.
3. Sonia Y, Neelam V, Vinod G, Rajput A, Maratha S. Oxadiazole and their synthetic analogues: An updated review. *Int J Pharm Biol Arch* 2018;9:4-9.
4. Revathy S, Amrutha U, Sneha J. Pharmacological activities of 1, 3, 4-oxadiazole derivatives: A review. *Res J Pharm Biol Chem Sci* 2017;8:468-88.
5. Asif M. A mini review on pharmacological activities of oxadiazole and thiadiazole compounds. *Mor J Chem* 2014;2:70-84.
6. Pitasse-Santos P, Sueth SV, Marco EF. 1,2,4- and 1,3,4-Oxadiazoles

- as scaffolds in the development of antiparasitic agents. *J Braz Chem Soc* 2018;29:435-56.
7. Glomb T, Szymankiewicz K, Swiatek P. Anti-cancer activity of derivatives of 1, 3, 4-oxadiazole. *Molecules* 2018;23:1-16.
 8. Irfan R, Matloob A, Zulfiqar AK, Mansha A, Maqbool T, Zahoor AF, *et al.* Recent advancements in oxadiazole-based anticancer agents. *Trop J Pharm Res* 2017;16:723-33.
 9. Marina T, Vera S, Alexandra B, Romanycheva A, Sharonova T, Baykov S, *et al.* An efficient synthesis and antimicrobial evaluation of 5-alkenyl- and 5-styryl- 1, 2, 4-oxadiazoles. *Arxivoc Part* 2018;7:1-13.
 10. Sunusi HH, Vivek G, Rakesh N. Synthesis and antibacterial activity of novel 3-[5-(4-substituted) phenyl-1,3,4-oxadiazole-2yl]-2-styrylquinazolin-4(3H)-ones. *J Pharm Res* 2017;9:1122-6.
 11. Paranjee K, Gopal L, Khatik. Identification of novel 5-styryl-1, 2, 4-oxadiazole/triazole derivatives as the potential anti-androgens through molecular docking study. *Int J Pharm Pharm Sci* 2016;8:72-7.
 12. Valentina P, Ilango K, Deepthi M, Harusha P, Pavani G, Sinddhura KL, *et al.* Antioxidant study of some substituted 1,2,4-triazo-5-thione Schiff bases. *J Pharm Sci Res* 2009;2:74-7.
 13. Glomb T, Szymankiewicz K, Piotr S. Anti-cancer activity of derivatives of 1, 3, 4-oxadiazole. *Molecules* 2018;23:3361.
 14. Ahsan MJ, Rathod VP, Singh M, Sharma R, Jadav SS, Yasmin S, *et al.* Synthesis, anticancer and molecular docking studies of 2-(4-chlorophenyl)-5-aryl-1,3,4-oxadiazole analogues. *Med Chem* 2013;3:294-7.
 15. Dhawan S, Kerru N, Awolade P, Singh-Pillay A, Saha ST, Kaur M, *et al.* Synthesis, computational studies and antiproliferative activities of coumarin-tagged 1,3,4-oxadiazole conjugates against MDA-MB-231 and MCF-7 human breast cancer cells. *Bioorg Med Chem* 2018;26:5612-3.
 16. James ND, Caty A, Payne H, Borre M, Zonnenberg BA, Beuzeboc P, *et al.* Final safety and efficacy analysis of the specific endothelin A receptor antagonist zibotentan (ZD4054) in patients with metastatic castration-resistant prostate cancer and bone metastases who were pain-free or mildly symptomatic for pain: A double-blind, placebo-controlled, randomized Phase II trial. *Drug Safety Res Unit* 2010;106:966-73.
 17. Andrew F, Peter P. P-glycoprotein and its role in drug-drug interactions. *Aust Prescr* 2014;37:137-9.
 18. Soumya J, Padmini K, Ruthu M, Rajitha G. Synthesis and evaluation of novel 5-(1-benzoyl amino-2-(substituted phenyl) vinyl)-2-amino-1,3,4-oxadiazoles for antimicrobial and antioxidant activities. *J Chem Pharm Res* 2012;4:4545-9.
 19. Venkanna A, Siva B, Poornima B, Vadaparathi PR, Prasad KR, Reddy KA, *et al.* Phytochemical investigation of sesquiterpenes from the fruits of *Schisandra chinensis* and their cytotoxic activity. *Fitoterapia* 2014;95:102-8.
 20. Aline AB, Michel MM, Margareth LA. Technical evaluation of antioxidant activity. *Medchem* 2014;4:517-22.
 21. Sreejayan N, Rao MN. Nitric oxide scavenging by curcuminoids. *J Pharm Pharmacol* 1997;49:105-7.
 22. Roberta R, Pellegrini N, Proteggente A, Pannala A, Yang M, Rice-Evans C, *et al.* Antioxidant activity applying an improved ABTS radical cation decolorization assay. *Free Radic Biol Med* 1999;26:1231-7.
 23. Grosdidier A, Zoete V, Michielin O. Swiss dock, a protein-small molecule docking web service based on Eadock DSS. *Nucleic Acids Res* 2011;39:270-7.
 24. Bhat KS, Karthikeyan MS, Holla BS, Shetty NS. Synthesis of some new fluorine containing 1, 3, 4-oxadiazole derivatives as potential antibacterial and anticancer agents. *Indian J Chem* 2004;43B:1765-9.
 25. Khalil NA, Kamal MA, Emam SH. Design, synthesis, and antitumor activity of novel 5-pyridyl-1, 3, 4-oxadiazole derivatives against the breast cancer cell line MCF-7. *Biol Pharm Bull* 2015;38:763-73.
 26. Yadav N, Kumar P, Chhikara A, Chopra M. Development of 1,3,4-oxadiazole thione based novel anticancer agents: Design, synthesis and *in-vitro* studies. *Biomed Pharmacother* 2017;95:721-30.
 27. Ozdemir A, Sever B, Altıntop MD, Temel HE, Atlı Ö, Baysal M, *et al.* Synthesis and evaluation of new oxadiazole, thiadiazole, and triazole derivatives as potential anticancer agents targeting MMP-9. *Molecules* 2017;22:1-15.
 28. Xin YB, Li JJ, Zhang HJ, Ma J, Liu X, Gong GH, *et al.* Synthesis and characterization of (Z)-styrylbenzene derivatives as potential selective anticancer agents. *J Enzyme Inhib Med Chem* 2018;33:1554-64.
 29. Andreani A, Granaiola M, Locatelli A, Morigi R, Rambaldi M, Varoli L, *et al.* Cytotoxic activities of substituted 3-(3,4,5-trimethoxybenzylidene)-1,3-dihydroindol-2-ones and studies on their mechanisms of action. *Eur J Med Chem* 2013;64:603-12.
 30. Negi AS, Gautam, Alam S, Chanda D, Luqman S, Sarkar J, *et al.* Natural antitubulin agents: Importance of 3, 4, 5-trimethoxyphenyl fragment. *Bioorg Med Chem* 2015;23:373-89.
 31. Starcevic K, Kralj M, Ester K, Sabol I, Grce M, Pavelić K, *et al.* Synthesis, anti-viral and anti-tumor activity of 2-substituted-5-amidino-benzimidazoles. *Bioorg Med Chem* 2007;15:419-42.
 32. Lipinski CA, Lombardo F, Dominy BW, Feeny PJ. Experimental and computational approaches to estimate solubility and permeability in drug discovery and development settings. *Adv Drug Deliv Rev* 2001;46:3-26.
 33. Lipinski CA. Lead-and Drug- like compounds: The rule-of- five revolution. *Drug Discov Today Technol* 2004;1:337-41.
 34. Amin ML. P-glycoprotein inhibition for optimal drug delivery. *Drug Target Insights* 2013;7:27-34.
 35. Roy SS, Vadlamudi RK. Role of estrogen receptor signaling in breast cancer metastasis. *Int J Breast Cancer* 2012;654698:1-8.
 36. Mukherjee S, Majumder D. Computational molecular docking assessment of hormone receptor adjuvant drugs: Breast cancer as an example. *Pathophysiology* 2009;16:19-29.
 37. Freudenberg JA, Wang Q, Katsumata M, Drebin J, Nagatomo I, Greene MI. The role of HER2 in early breast cancer metastasis and the origins of resistance to HER2-targeted therapies. *Exp Mol Pathol* 2009;87:1-11.